REVIEW

Study of the Role of Nitrogen in the Oxidation of Titanium-Based Alloys by Changing the Reaction Gas

Kevin Gautier[1] · Daniel Monceau[1] · Enrica Epifano[1] · Damien Connétable[1] · Thomas Gheno[2]

Abstract

The role of nitrogen in the oxidation of Ti-2W, Ti-10Al-2W (at.%) and Ti6242S was investigated using experiments in air and in Ar-20%O_2, and two-stage experiments where the reaction gas was switched from one mixture to the other. When switching from Ar-20%O_2 to air, the oxidation rates first increased during a short period, then decreased. This surge of mass gain following the introduction of air was attributed to N pickup, forming a nitride layer and a N-enriched zone in the alloy, below the oxide layer. The subsequent decrease of oxidation rate was attributed to the formation of nitride and/or N-rich zone, which both act as diffusion barriers for oxygen. Switching from air to Ar-20%O_2 caused an increase in the oxidation rate of the W-containing alloys, which was attributed to the consumption of this barrier. The gas change had no significant effect on the oxidation rate of Ti6242S, which formed a much thinner nitride layer in air. The faster the nitride layer grows, the faster it is consumed when removing N from the reaction gas, probably because of a higher diffusion rate of N in W-doped TiO_2 compared to TiO_2 formed on Ti6242S.

✉ Kevin Gautier
kevin.gautier@toulouse-inp.fr

Daniel Monceau
daniel.monceau@toulouse-inp.fr

[1] CIRIMAT, Université de Toulouse, CNRS, INPT, 4 allée Emile Monso, BP44362, 31030 Toulouse Cedex 4, France

[2] DMAS, ONERA, Université Paris-Saclay, 92322 Châtillon, France

🙂 Springer

Introduction

Owing to their high specific mechanical properties, titanium alloys compete with nickel-based alloys for applications in aircraft engines. Nevertheless, the uses of these alloys are limited to moderate temperatures (below about 500 °C) because of insufficient creep resistance and oxygen embrittlement resulting from high-temperature oxidation. This embrittlement is due to the oxygen uptake in titanium alloys, which can dissolve much more oxygen (about 33 at.% in α-Ti [1]) than the concentration of the brittle-to-ductile transition induced by oxygen (below 1 at.% in Ti64 [2] and 0.5 at.% in Ti6242S [3]). In addition to oxygen dissolution and diffusion leading to an oxygen-affected zone (OAZ), titanium alloys also form an oxide scale, mainly composed of rutile TiO_2. This oxide is commonly about 5–10 times thinner than the OAZ [4].

One of the most studied ways to reduce the O uptake is to add alloying elements. Previous studies have shown that some elements such as niobium [5] or silicon [6, 7] strongly decrease the scaling rate, but do not affect the O enrichment in the alloy. The addition of aluminum decreases both the scaling rate and the O diffusivity [8, 9]. Tungsten is used to improve the creep resistance of Ti alloys [10]. Moreover, we recently showed that this element strongly decreases the oxidation rate in air by decreasing scale thickening and oxygen dissolution [9]. It was shown that this decrease is due to the formation of a continuous layer of titanium nitride Ti_2N below the oxide scale. It should be noted that the beneficial effects of tungsten disappear during oxidation in Ar-20%O_2.

The effect of nitrogen on the oxidation of Ti alloys has mostly been studied by comparing results obtained in air and in Ar-20%O_2 [5, 6, 9, 11–14]. Nitrogen uptake on pure titanium at 700 °C was analyzed by nuclear reaction analysis (NRA), which amounted to about 16% of the total mass gain [15]. The oxidation rate is lowered by the presence of nitrogen in the reaction gas. Three possible explanations to the effect of nitrogen on Ti and Ti-X alloys (with Si, Cr and Al) were proposed by Chaze et al. [11]. Since oxide scales formed in air are thinner than those formed in O_2, they consider that nitrogen could be incorporated in the rutile layer and could decrease the oxygen vacancy concentration. The second proposed explanation is the decrease of O solubility by N dissolution in the metal. Dupressoire et al. analyzed a Ti6242S alloy oxidized at 650 °C for 1000 h in air by atom probe tomography (APT) and transmission electron microscopy (TEM), and found a N-rich layer with a very low O concentration (about 1 at.%) below the oxide scale [12]. The third explanation is the formation of nitrides at the oxide/metal interface, which we identified in W-containing alloys in our previous study [9]. Therefore, we posit that the lower oxidation rate observed for Ti–W and Ti–Al-W alloys in air, compared to Ar-20%O_2, is due to both the formation of a continuous nitride layer and to the decrease of the oxygen solubility in the N-rich layer beneath the oxide scale [9]. To examine this hypothesis, oxidation experiments were conducted by changing the reaction gas from Ar-20%O_2 to air and conversely.

Experimental Procedures

Materials

Tungsten-containing model alloys were fabricated in an electric arc furnace (see experimental details in [9]). Their compositions were measured by inductively coupled plasma-optical emission spectroscopy (Spectro Ciros) for the major elements and by fusion/gas analysis (Inductar) for oxygen and nitrogen. The results are listed in Table 1. These compositions were chosen to obtain near-α alloys. The solubility of W in the α phase is very low (maximum 0.20 at.% at 740 °C) [16], but adding small quantity of W does not change significantly the β fraction. Tungsten was added in small quantities to avoid an excessive increase in alloy density. Aluminum was also added due to its presence in almost all Ti-based alloys and because it stabilizes α-Ti. Experiments were also performed on wrought Ti6242S as a reference commercial alloy for high-temperature use. The amount of native oxygen and nitrogen in Ti6242S was measured by fusion/gas analysis at Eurofins EAG Laboratories (Tournefeuille, France), and the results are included in Table 1. The microstructure of the model alloys mostly consists of lamellar α phase with very small β fraction (about 2 vol.%). The microstructure of Ti6242S is duplex, composed of lamellar and globular α-phase in a β-phase matrix (see observations in ref [9]). Vande Put et al. showed that the microstructure of the Ti6242S alloy had no effect on the overall mass gain and oxygen dissolution rates for a given β fraction [17]. The same observation was done for Ti64 alloy [18]. Nevertheless, a large amount of β may affect the oxidation kinetics as the oxygen solubility and diffusivity are different in α and β phases [1, 19].

Samples for oxidation experiments were cut from ingots as thin plates of approximately $13 \times 8 \times 2$ mm^3, and a 2.5 mm diameter hole was drilled for suspension using an alumina rod. Prior to oxidation, the samples were ground using P600 SiC papers on the faces, edges and corners to limit scale spallation. They were finally cleaned in ethanol in an ultrasonic bath and dried in air. The samples were weighed three times using a SARTORIUS LA75 3200D balance with an accuracy of ± 20 µg.

Experiments and Characterization

Oxidation tests were carried out at 650 °C in three different apparatus. Interrupted tests in laboratory air were performed in a CARBOLITE CWF1300 furnace with natural convection. The experiment was interrupted for weighing at intermediate exposure times. Interrupted tests in Ar-20%O$_2$ were performed in an oxidation

Table 1 Alloy compositions, in atomic percent (at.%)

Alloy	Ti	Al	Zr	Mo	Sn	Si	W	O	N
Ti-2W	base	–	–	–	–	–	2.0	0.38	0.01
Ti-10Al-2W	base	9.7	–	–	–	–	2.1	0.51	0.01
Ti6242S	base	10.5	2.1	1.0	0.7	0.2	–	0.228	0.009

bench with a gas velocity of 1.2×10^{-4} m.s^{-1}, corresponding to a gas flux of 51 mL.min^{-1}. Continuous weighing tests with changes in the reaction gas between synthetic air and Ar-20%O$_2$ were carried out in a SETARAM TAG24s thermobalance, which has an excellent mass stability over time (better than 0.5 μg/h). Heating and cooling rates were set at 60 °C.min^{-1}. The reaction gas was switched at high temperature by pumping the old gas out down to 2×10^{-2} mbar, and then filling the reaction chamber with the new gas at 200 mL.min^{-1}. This operation took 15 min. Oxidation during the filling can presumably be neglected. The difference of buoyancy between air and Ar-20%O$_2$ can also be neglected (about 0.01 mg.cm^{-2}). After the filling operation, the gas flux was set to 20 mL.min^{-1}, corresponding to a gas velocity of 1.0×10^{-3} m.s^{-1}.

After oxidation, copper was electrodeposited on the samples to protect the oxide layer. Cross sections were then cut, mounted, ground with P600 and P1200 SiC paper and then automatically polished down to 1 μm diamond solution. They were rinsed with water between each diamond solution, cleaned into ethanol under ultrasounds and dried in air. The polished sections were observed using a FEI Quanta 450 Scanning Electron Microscope (SEM) and a JEOL JSM 7800F Prime FEG-SEM. From the cross-sectional SEM images, the oxide or nitride scale thicknesses were measured by calculating the ratio between the oxide/nitride surface area and the length of the oxide scale.

Results

From Ar-20%O$_2$ to Air

Experiments with a change of reaction gas from Ar-20%O$_2$ to air were performed to examine the influence of nitrogen on pre-oxidized samples. Samples were first oxidized in Ar-20%O$_2$ during 16 h, and then in air during 30 h. The mass changes obtained by thermogravimetry are shown in Fig. 1a (solid lines). The blue dashed line corresponding to a change of gases after only 10 h for Ti-2W alloy. When switching from Ar-20%O$_2$ to air, the oxidation rates first increase during a short period of time, and then decrease to reach a lower value than in Ar-20%O$_2$. The mass change followed parabolic kinetics in each sample, before and after the change of reaction gas. The kinetics were analyzed using the complete parabolic law [20]:

$$t = A + B\left(\frac{\Delta m}{S}\right) + \frac{1}{k_p}\left(\frac{\Delta m}{s}\right)^2 \tag{1}$$

where A and B are coefficients which depend on interfacial reaction kinetics and on the transient regime before the pure parabolic regime and k_p the parabolic rate constant. Table 2 gives the parabolic constants k_p before and after the change of reaction gas obtained by fitting Eq. 1 to the experimental data. In Ar-20%O$_2$, the oxidation rate of Ti-2W is much higher than that of Ti-10Al-2W and Ti6242S, as already reported in our previous study [9].
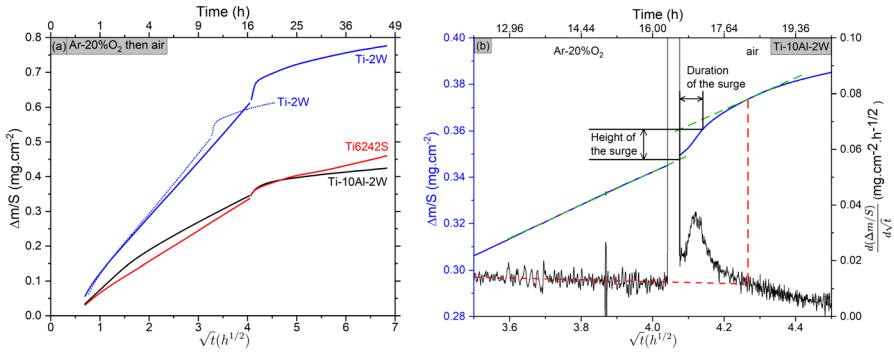
Fig. 1 **a** Sample mass gain versus square root of time for Ti-2W (blue lines), Ti-10Al-2W (black line) and Ti6242S (red line) oxidized at 650 °C for 16 h in Ar-20%O_2 and 30 h in air (solid lines), or for 10 h in Ar-20%O_2 and 10 h in air (dot line). **b** Zoom on Ti-10Al-2W: in blue, mass gain versus square root of time, and in black, the derivative of the blue line versus the square root of time

Table 2 Parabolic rate constants $k_p[10^{-7} \text{ mg}^2 \cdot \text{cm}^{-4} \cdot \text{s}^{-1}]$ for each sample before and after the change of reaction gas

Alloys	k_p before the change (Ar-20%O_2)	k_p after the change (air)	(k_p Ar-20%O_2)/ (k_p air)
Ti-2W	83 ± 3 [0–10 h]	1.4 [11–20 h]	59
	72 ± 5 [0–16 h]	1.5 [17–30 h]	48
Ti-10Al-2W	15 ± 4 [0–16 h]	0.3 [18–30 h]	50
Ti6242S	22 ± 2 [0–16 h]	1.9 [18–30 h]	12

Table 3 Height and duration of mass change surge following the gas change. The oxide scale thicknesses were estimated from our previous study [9]

Alloy	Height of the surge (mg. cm^{-2})	Duration of the surge (min)	Oxide scale thickness at the reaction gas change (μm)
Ti-2W (10 h)	0.027	13.2	1.55
Ti-2W (16 h)	0.031	26.4	1.81
Ti-10Al-2W	0.012	30.4	1.04
Ti6242S	0.015	11.6	0.94

After the change of reaction gas, the k_p value of Ti6242S is the highest. The oxidation rates of the W-containing alloys are the most affected by the change of reaction gas. Indeed, the k_p ratios for these alloys are much higher than that measured for Ti6242S (Table 2).

An increase in the oxidation rate is observed for a short period after the change of reaction gases in Fig. 1a. Table 3 gives heights and durations of this mass gain surge. The main characteristics of the surge are defined as follows. The derivative

of the mass gain before the change is extrapolated to longer durations until it intersects the derivative curve after the gas change (in red in Fig. 1b). This gives the time required to reach the same instantaneous oxidation rate as before the change. The tangent of the mass gain curve before the change (in green in Fig. 1b) is extended to the end of the gas change in the thermobalance. The height of the surge is defined as the difference in mass between the extensions of the green curves in Fig. 1b. The duration of the surge is defined by the duration between the end of the gas change and the time when the mass gain derivative curve reaches its top (Fig. 1b).

The increase of oxidation rate appeared very quickly in each case, in less than a dozen of minutes after the end of the furnace's filling. The surge is the highest for Ti-2W and the shortest for Ti6242S. The surge lasts up to half an hour for Ti-10Al-2W. Table 3 also gives the oxide scale thickness at the gas transition, calculated from data obtained in a previous study [9]. It should be noticed that there is a correlation between the thickness of the oxide scale and the height of the surge.

Titanium nitrides Ti_2N was identified by cross-sectional SEM imaging (Fig. 2) below the oxide scale in Ti-2W, and confirmed by XRD (not presented here), but no nitrides was identified on SEM images in Ti-10Al-2W and Ti6242S. The other phases identified by XRD were the α matrix and rutile TiO_2, which were common across all the samples.

From Air to Ar-20%O_2

Figure 3a shows the mass gain obtained by discontinuous weighing for oxidation with a change from air to Ar-20%O_2. Data obtained from single-gas experiments in our previous study [9] are shown for comparison.

We first note the good reproducibility of the oxidation rates obtained in air. At the end of the oxidation test in air, a layer of titanium nitrides was observed under the oxide scale in Ti-2W and Ti-10Al-2W, but not in Ti6242S [9]. Dupressoire et al. evaluated the nitride thickness in a Ti6242S alloy oxidized at 650 °C for 1000 h between twenty and a hundred of nanometers [12].

Figure 3a shows that the oxidation rate of the W-containing alloys increases by several dozen hours after changing the reaction gas. The delay after the change is comprised between 50 and 120 h. No change of oxidation rate was observed for Ti6242S. Table 4 gives the k_p values before and after the change of reaction gas, with the comparison of oxidation rates obtained in single-gas experiments in our previous work [9]. Oxidation rates obtained after the change of reaction gas are very close
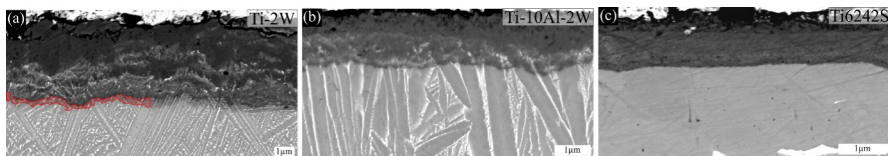

Fig. 2 SEM-FEG images (BSE mode) of oxide scales for alloys oxidized at 650 °C for 16 h in Ar-20%O_2 and 30 h in air for **a** Ti-2W, **b** Ti-10Al-2W and **(c)** Ti6242S. Red area in **(a)** indicates the nitride Ti_2N
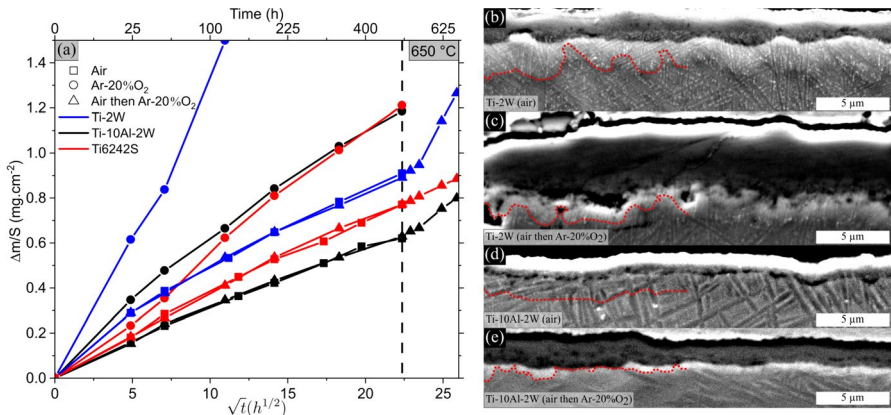
Fig. 3 a Sample mass gain versus square root of time for Ti-2W (blue line), Ti-10Al-2W (black line) and Ti6242S (red line) oxidized at 650 °C for 500 h in air (squares), for 500 h in Ar-20%O$_2$ (circles) and 500 h in air followed by 170 h in Ar-20%O$_2$ (triangles). **b–e** SEM images (secondary electron SE mode) of oxide and nitride layers for Ti-2W **b and c** and Ti-10Al-2W **d and e** before the change **b and d** and after the change **c, e** of reaction gas. Red dotted lines indicate the nitride/metal interface

to those obtained previously for oxidation only in Ar-20%O$_2$, except for Ti6242S which follows the same oxidation kinetics as in air. Cross-sectional observations, presented in Fig. 3b-e, show the evolution of the nitride layer after 500 h in air and after an additional 170 h in Ar-20%O$_2$. Ti6242S observations are not presented due to the absence of visible nitrides. A considerable decrease of nitride thickness is visible, to such an extent that the continuity of the nitride layer is lost in the two alloys.

Discussion

From Ar-20%O$_2$ to Air

The surge observed after switching from Ar-20%O$_2$ to air is necessarily due to nitrogen. There are three possible contributions to the mass gain associated with this surge: nitrogen dissolution in the oxide scale, nitrogen in a nitride layer and nitrogen dissolution in the metal. The first assumption cannot be valid, as the excess of mass would correspond to a very high concentration of nitrogen in the oxide (about 10 wt.% N in TiO$_2$), which was never observed experimentally. Moreover, there is no significant difference between the surge heights observed for the same alloy (Ti-2W) when the gas change was performed at two different oxide scale thicknesses (after 10 or 16 h), which dismisses the hypothesis that the excess mass is due to N dissolution in the oxide. Concerning the dissolution of N in the metal, by integration of the concentration profile obtained after 1 h at 650 °C (given a N diffusivity of about 8×10^{-18} m^2.s^{-1} [21, 22]), and assuming a concentration at the oxide/metal interface equal to 20 at.% (as measured by APT and TEM-EDS in Ti6242S [12]), the mass gain from nitrogen dissolution in α-Ti is estimated to be about 0.01 mg.

Table 4 Parabolic rate constants k_p [10^{-7} mg$^2 \cdot$ cm$^{-4} \cdot$ s^{-1}] for each sample before and after the change of reaction gas. Isothermal values from single-gas experiments in Gautier et al. were added for comparison [9]

Alloys	Ti-2W	Ti-10Al-2W	Ti6242S	Ti-2W [9]	Ti-10Al-2W [9]	Ti6242S [9]
k_p before the change (air)	3.1 [0–500 h]	1.8 [0–500 h]	2.8 [0–500 h]	5.6 [0–200 h] 2.1 [200–2500 h]	2.1 [0–200 h] 0.8 [200–5000 h]	2.7 [0–1000 h]
k_p after the change of slope (Ar-20%O$_2$)	47 [620–670 h]	8.4 [620–670 h]	3.0 [500–670 h]	50 [0–120 h]	8.9 [0–500 h]	8.4 [0–500 h]

cm^{-2}. This value is consistent with the surge heights measured for Ti-10Al-2W and Ti6242S. This suggests that the excess mass could be due to N dissolution in α-Ti. In the case of Ti-2W, however, the excess mass is larger. We conclude that the surge reflects both N in the nitride layer and N dissolution in the metal. The average thickness of titanium nitrides in Fig. 2a is about 250 nm, which corresponds to a mass gain of N of about 0.02 $mg.cm^{-2}$. This value is consistent with the difference between the measured excess and the estimated nitrogen dissolution in the alloy.

The subsequent decrease in oxidation rates could be due to the formation of nitrides, which acts as an oxygen diffusion barrier. Oxygen and nitrogen fit into the same interstitial sites (octahedral sites) in α-Ti [23]. There is therefore a competition in the dissolution of these species, as shown in [12]. The species that diffuses the slowest (N) accumulates at the oxide–metal interface, and occupies octahedral sites where O can no longer enter. This layer enriched in N is thus expected to act as an O diffusion barrier.

Figure 4 schematically illustrates the evolution of oxygen and nitrogen concentration at each major step of the reaction process. Before the reaction gas change (1 in Fig. 4), the mass gain stems from two contributions: oxide scale growth and oxygen enrichment in the alloy. After the change from Ar-20%O_2 to air, nitrogen diffuses also through the oxide scale and accumulates in the alloy just beneath the oxide scale by replacing O (2 in Fig. 4). This can lead to the precipitation of a nitride layer (3a in Fig. 4), as seen in Ti-2W alloy, or not (3b in Fig. 4). As oxidation continues in air, the mass gain stems from oxide growth, nitride growth when applicable and O and N enrichment in the alloy. The presence of the nitride layer and of an N-enriched zone in the alloy both contribute to reducing oxygen dissolution in the alloy and overall mass gain.

From Air to Ar-20%O_2

As described in the Results section, the oxidation rate increases several dozen hours after the gas is changed from air to Ar-20%O_2. This is consistent with the loss of continuity of the nitride layer, observed in Fig. 3c and e. Note that in air or in Ar-20%O_2, the oxide grows by oxidizing the nitride layer when present [15]. In air, the
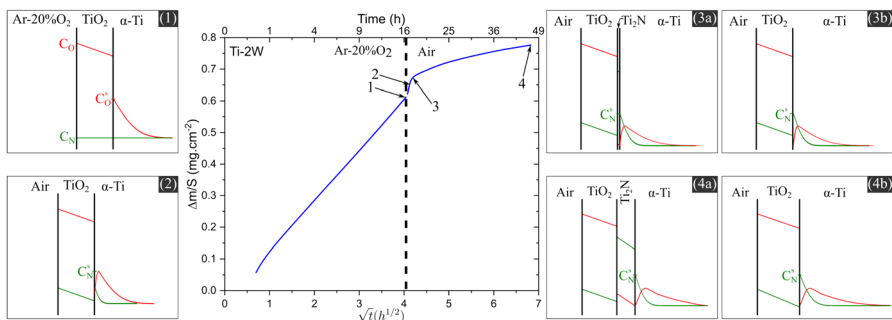

Fig. 4 Schematics of the evolution of oxygen and nitrogen concentration in each scale depending on time for Ti-2W oxidized at 650 °C for 16 h in Ar-20%O_2 and 30 h in air

nitrogen released by the nitride oxidation is in a chemical potential gradient which makes it diffuse through the nitride layer to grow the nitride at the nitride/α-Ti interface (Fig. 5a). During further oxidation in Ar-20%O_2, the oxidation of the nitride layer continues to release N. However, the large decrease of N partial pressure in the gas (the Ar-20%O_2 gas mixture may contain very low N impurities) is expected to reverse the chemical potential gradient in the oxide scale (Fig. 5b and c). Nitrogen may then diffuse either through the oxide scale toward the gas and exit the sample, or through the nitride layer toward the alloy if there is a local supersaturation at the oxide/nitride interface.

In air, the growth of the nitride scale is controlled by the lowest N flux between the oxide and the nitride. In air, oxide scales thicknesses of Ti-10Al-2W and Ti6242S are similar (1.4 µm vs. 1.1 µm from our previous study [9]). Yet, the nitride layer is much thicker in Ti-10Al-2W than in Ti6242S, referring to Dupressoire et al. who identified a nitride layer of about 10 to 100 nm thickness after 1000 h at 650 °C in Ti6242S [12]. Assuming a constant value of N diffusivity into the nitride for all alloys, this result shows that the N diffusivity in the oxide is lower for Ti6242S than for Ti-10Al-2W.

As argued in the Results section, the increase of oxidation rates following the switch to Ar-20%O_2 is due to a loss of continuity of the nitride layer. This increase is observed for the model alloys but not for Ti6242S. Based on these results, the question which arises is which diffusion mechanism is the limiting step of nitride consumption. Three different processes can be the limiting step: O or N diffusion through the oxide scale, or N diffusion through the nitride. The nitride dissolution at the nitride/metal interface is not considered due to the low N diffusivity in the α phase. Ti-10Al-2W and Ti6242S have almost the same oxidation rates in Ar-20%O_2 (Fig. 3a) with similar oxide scale thicknesses (3.6 µm vs. 3.4 µm from our previous study [9]). We conclude that the kinetics of nitride consumption is not controlled by O diffusion in the oxide for these two alloys. On the contrary, this is likely the controlling mechanism for Ti-2W, for which the O diffusivity through the oxide scale is higher than for the other alloys. This induces a fast nitride consumption rate for Ti-2W, and the released N exits the sample through the oxide scale due to a higher outward flux of N compared to the inward flux. For Ti-10Al-2W and
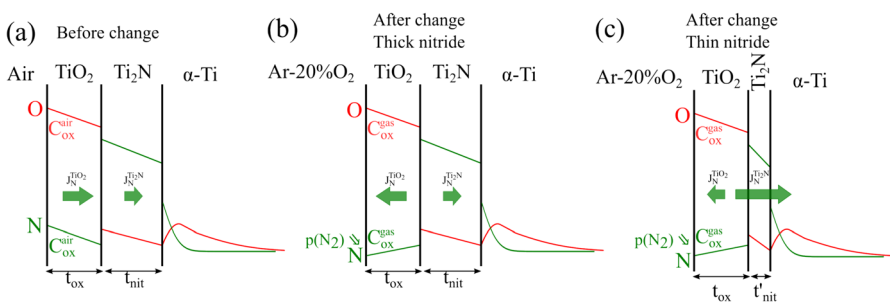

Fig. 5 Oxygen and nitrogen concentration profiles **a** before the change (in air), **b** after the change with a thick nitride (like Ti-2W and Ti-10Al-2W) leading to nitride consumption, **c** after the change with a thin nitride (like Ti6242S)

Ti6242S, assuming a constant value of N diffusivity in the nitride for all alloys, the flux of N through the nitride layer is higher in a thinner nitride (Ti6242S) than in the thicker nitride (Ti-10Al-2W). As said before, the N diffusivity in the oxide is lower for Ti6242S than for Ti-10Al-2W. There is therefore a competitive effect between the inward N diffusion through the nitride and the outward N diffusion through the oxide, illustrated in Fig. 5b and c. In Ti-10Al-2W, the outward N flux is higher than the inward flux, leading to a large nitride consumption and thus to the increase of k_p with increasing O uptake. In Ti6242S, the inward diffusion of N which leads to the growth of the nitride layer at the nitride/alloy interface is higher than the outward diffusion through the oxide scale, leading to a limited nitride consumption. The O diffusion barrier and the mass gain kinetics are maintained. All these results can be summarized as "if the nitride growth is fast, its consumption is fast as well."

Conclusion

Oxidation tests with changes of reaction gases were performed at 650 °C on three different alloys (Ti-2W, Ti-10Al-2W and Ti6242S), in order to better understand how nitrogen influences the oxidation mechanism in titanium alloys. It was shown that when switching from Ar-20%O_2 to air, the decrease in the oxidation rate is preceded by an increase in the rate lasting less than one hour. This increase in mass was attributed to nitrogen uptake in the metal below the oxide scale, and the duration of the surge was attributed to the time needed to reach nitrogen saturation in the alloy below the oxide scale.

Nitride formation was observed only in the Ti-2W alloy. In the Ti-10Al-2W alloy, no nitride layer was observed. Two explanations are possible: either a nitride layer formed but was too thin to be observed by SEM, or the zone below the oxide scale saturated in nitrogen acted as a diffusion barrier for oxygen, explaining the decrease in the oxidation rate. The switch from air to Ar-20%O_2 showed an increase in the oxidation rate for W-containing alloys. This is consistent with the loss of continuity of the nitride layer due its fast oxidation. The nitride layer is oxidized quickly in W-enriched alloy because of the high diffusivity of the released nitrogen through the oxide scale. Conversely, the absence of any visible change in Ti6242S after switching from air to Ar-20%O2 indicates the preservation of the effectiveness of the oxygen diffusion barrier. This may be due to the fact that nitrogen diffusion is slow in the oxide grown on Ti6242S. The nitrogen produced at the oxide/nitride interface during nitride oxidation is more prone to diffuse inward through the thin nitride than outward through the oxide layer.

Author contribution D.M took part in the conception of the work. All authors participated in the interpretation of data. K.G wrote the main manuscript text and prepared all the figures. All authors reviewed the manuscript.

Data availability No datasets were generated or analyzed during the current study.

Declarations

Conflict of interests The authors declare that they have no known competing financial interests or personal relationships that could have appeared to influence the work reported in this paper.

References

1. H. Okamoto, *Journal of Phase Equilibria and Diffusion* **32**, 473 (2011).
2. Antoine Casadebaigt, Jonathan Hugues, and Daniel Monceau, *Corrossion Science* **175**, 108875 (2020).
3. R. N. Shenoy, J. Unnam, and R. K. Clark, *Oxid. Met.* **26**, 105–124 (1986).
4. N. Vaché, Y. Cadoret, B. Dod, and D. Monceau, *Corrosion Science.* **178**, 109041 (2021).
5. M. Gobel, V. A. C. Haanappel, and M. F. Stroosnijder, *Oxid. Met.* **55**, 137 (2001).
6. A. M. Chaze and C. Coddet, *Metals.* **27**, 1 (1987).
7. T. C. Valenza, P. Chao, P. K. Weber, O. K. Neill, and E. A. Marquis, *Corrosion Science* **217**, 111110 (2023).
8. A. M. Chaze and C. Coddet, *Journal of the Less-Common Metals.* **157**, 55 (1990).
9. K. Gautier, E. Epifano, T. Gheno, D. Connétable, and D. Monceau, Effect of refractory alloying elements (W, Ta and Hf) on oxidation kinetics and oxygen dissolution and diffusion in titanium alloys. *Corrosion Science* (2024, in press).
10. Z. Huvelin, C. Gouroglian, N. Horézana, and S. Naka, Role of refractory elements in near-alpha titanium alloys on high temperature mechanical properties. *MATEC Web of Conferences*. **321**, 04018 (2020).
11. A. M. Chaze and C. Coddet, *Journal of the Less Common Metals.* **124**, 73 (1986).
12. C. Dupressoire, M. Descoins, A. Vande Put, et al., *Acta Materialia.* **216**, 117134 (2021).
13. R. J. Hanrahan and D. P. Butt, *Metals.* **47**, 317 (1997).
14. R. J. Hanrahan and D. P. Butt, *Metals.* **48**, 41 (1997).
15. V. Optasanu, P. Berger, M. C. Marco de Lucas, et al., *Corrosion Science* **216**, 111072 (2023).
16. Z.-p Jin and C. Qiu, *Materials Science and Technology.* **9**, 378 (1993).
17. A. Vande Put, C. Dupressoire, C. Thouron, et al., *Metals.* **96**, 373 (2021).
18. Casadebaigt A, Monceau D, Hugues J. High Temperature Oxidation of Ti-6Al-4V Alloy Fabricated by Additive Manufacturing. Influence on Mechanical Properties *MATEC Web Conf.* **321**, 03006 (2020)
19. C. J. Rosa, *Metallurgical Transactions.* **1**, 2517 (1970).
20. D. Monceau and B. Pieraggi, *Metals.* **50**, 477 (1998).
21. A. Anttila, J. Räisänen, and J. Keinonen, *Applied Physics Letters.* **42**, 498 (1983).
22. F. L. Bregolin, M. Behar, and F. Dyment, *Applied Physics A.* **90**, 347 (2008).
23. L. Scotti and A. Mottura, *The Journal of Chemical Physics.* **144**, 084701 (2016).